# MODIFICATION OF THE MASTER GENERATOR METHOD USED FOR FREQUENCY AND VOLTAGE CONTROL IN ISOLATED POWER SYSTEMS WITH PARALLEL OPERATING AC GENERATORS

**L.I. Mazurenko[1]\*, O.V. Dzhura[1]\*\*, M.O. Shykhnenko[1]\*\*\*, A.V. Kotsiuruba[2]\*\*\*\***
**¹ Institute of Electrodynamics of the National Academy of Sciences of Ukraine,**
**Peremohy Ave., 56, Kyiv, 03057, Ukraine.               E-mail:   3662491@gmail.com.**
**² Ivan Chernyakhovsky National Defense University of Ukraine,**
**Povitroflotsky Ave., 28, Kyiv, 03049, Ukraine.**

*Such methods as droop method, curve shifting method and master-slave method were primarily developed for voltage and frequency regulation in isolated power systems with synchronous generators. In modern power systems induction generators, regulated dump loads, energy storage devices with AC/DC and AC/DC/AC power converters, etc. are used in addition to synchronous generators. The investigation of new configurations of power systems is closely tied with further development of control methods for load sharing and regulation of voltage and frequency of the systems. The article reviews simple-to-implement known control methods used for control of isolated power systems with parallel operated synchronous generators and proposes a modification of the master-slave method for control of power systems with parallel operated synchronous and induction generators, static var compensators, dump loads and energy storage devices with interface power converters. The system "Hydroelectric unit with a synchronous generator - dump load - hydroelectric unit with an induction generator - compensating capacitors - transformer – AC local load" is considered and two techniques for regulation of electric frequency and voltage magnitude in the specified system are presented with accordance to the statements of the proposed modified method. The proposed control algorithm of the dump load frequency controller is in agreement with the control algorithm of the speed controller of the master unit. The functions assigned to the electronic PID speed controller of the master unit are to maintain the electric frequency in the system equal to nominal value and regulate the active power sharing. Verification of the proposed control algorithms for isolated electric power systems was carried out.* References 23, figures 5, table 1.
*Keywords:* isolated power system, method, master generator, slave generator, dump load.

**Introduction.** In order to improve the reliability of power supply to AC consumers powered by isolated power systems (IPSs), these systems are designed with parallel operated generators. IPSs are often equipped with diesel sets. Gas and hydraulic turbine driven electric generators is a good choice for an IPS when gas fuel and hydropower are available nearby. The construction of a hydraulic IPS requires more capital investments than for a diesel or diesel-battery system of comparable capacity. However, in the presence of hydro resources with required water head and flow, if stable power consumption is observed, preference should be given to a hydraulic IPS due to its independence of the fossil fuel. For a more optimal use of hydro resources, it is advisable to consider the possibility of building a hydro-wind IPS [1, 2]. The independence from the fossil fuel, lower cost of electricity production compared to diesel and wind-diesel power plants, and good predictability of hydro resources have caused the interest in problematic issues and searching approaches for improving technical characteristics of hydraulic IPSs.

Among various types of generators in electrical equipment of IPSs, as well as in centralized power systems, synchronous generators (SGs) with electromagnetic excitation are mostly preferred, but IPSs with permanent magnet generators and induction generators (IGs) are known as well [3-6]. The so-called doubly fed induction generators are used mainly in grid-tied variable frequency wind turbines [7]. However, their application is also possible in IPSs with power output from several megawatts and higher. In scientific papers devoted to the study of isolated and islanded hydraulic power stations (HPSs), HPSs with one

ORCID ID: * https://orcid.org/0000-0002-7059-249X; ** https://orcid.org/0000-0002-0224-3351;
*** https://orcid.org/0000-0003-4012-1731; **** https://orcid.org/0000-0001-5150-6683

hydroelectric unit are most often considered and somewhat less HPSs with two or more generators operating in parallel [8-12].

Connection of an IG with a SG supplying an asymmetric load for parallel operation provides the SG's current asymmetry reduction and, due to this, increases the operating life of the SG. The advantage of this solution is that the cost of the IG is lower than the SG of the same power, and the procedure for connecting the IG to the IPS is simpler than for the SG.

An important scientific task for IPS researchers is the development of methods and algorithms for controlling the parallel operation of generators. These methods and algorithms should ensure operation of IPSs only with allowed frequency and voltage magnitude deviations, the specified power distribution between the units and minimization of the power exchange between the generators.

The active power of a SG, as is known, is proportional to its load (power) angle – the angle between induced EMF and terminal voltage vectors of the stator winding. Regulation of this angle is made by changing the mechanical torque of the SG with a speed governor [13]. The active power of an IG is regulated in the same way.

The reactive power of a SG is proportional to the magnitude of the induced EMF and is controlled by changing the magnitude of the DC excitation current. Asynchronous machine with a short circuited rotor, both in the motoring and in the generating mode, as well known, needs a source of reactive power for magnetization. Possible reactive power sources are SG (or synchronous compensator), network, capacitors, static compensator [14-18].

Since IPSs, as noted, have been designed for a long time using parallel-connected SGs with electromagnetic excitation, then, accordingly, the control methods developed at that time for IPSs are primarily focused on AC IPSs with SGs operating in parallel [19, 20], and somewhat later found application in systems with energy resource interface inverters [21]. The best known of these methods are droop method (DM), curve shifting method (CSM) and master-slave method (MSM). In Soviet and post-soviet scientific works the DM is called as the method of static characteristics, the CSM is called as the method of imaginary static characteristics and the MSM is called as the master (main) generator method (MGM).

The DM is the most simple and known one among them. The application advantage of the DM is the informational independence of control systems of power supply units in the system. Since the input variables of frequency and voltage controllers of a unit in an IPSs with DM-based control are active and reactive output power signals of the unit, there is no need for informational communication between the units. Its main disadvantage is the use of static frequency and voltage regulators.

Frequency and voltage regulation in a system according to the CSM is actually performed due to the dynamic shifting of the voltage and frequency droop characteristics of the units. Its advantage is that it provides zero voltage and frequency steady state errors. But disconnection of any one of the generators from the system with CSM-based control and a passive (resistive) load will cause a reduction of the electrical frequency and voltage magnitude in the system after a transient.

According to the MGM, the regulation of voltage and frequency in the system is provided solely by the master unit (MU) with a SG. The advantage of the MGM over the DM is the zero voltage and frequency steady state errors, and its advantage over the CSM is the preservation of system operability when any of the generators is disconnected from the system except the master generator (MG). The disadvantage of the MGM is that when it is used, the quality of voltage and frequency regulation in the system depends mainly on characteristics of the MU. In addition, the MU during transients experiences increased loads due to the functions assigned to it. Therefore, there is a need to improve this method.

***The purpose*** of the article is to develop a modified master generator method for voltage and frequency regulation in IPSs with parallel operating AC generators and verify developed controllers for regulation of frequency and voltage in AC IPSs using a simulation model.

**Development of the modified master generator method.** To improve the quality of frequency and voltage regulation during transients in IPSs, it is proposed to modify the MGM by putting into use the principle of assistance to the master generator by other elements of the power supply system. Such a modified MGM (MMGM) can be applied for regulation of frequency and voltage in IPSs with parallel operated AC generators, electronic power converters, controlled resistive elements, battery inverters, etc.

An example of such a system is shown in Figure 1. The system is composed of two hydraulic units with regulated hydraulic turbines (HT1, HT2). The HT1 turbine rotates the SG (unit *1*) and the HT2 turbine rotates the IG (unit *2*). Unit 1 is the MU and unit 2 is the slave unit (SU). Mechanical torques of the HT1 and HT2 turbines are regulated by the wicket gate (WG) angles $c_1$ and $c_2$ control. The WGs are rotated by servo

motors. The SG and IG operate in parallel and supply local consumers through the transformer TR1. Additionally a regulated dump load (RDL) for frequency and "spinning" reserve regulation and compensating capacitors for decreasing of reactive power component of the SG output power are added. Development of simulation model of the Fig. 1 configuration affords testing of discussed below voltage and frequency regulators intended for AC IPSs.

The fundamentals of the MGM are illustrated by Fig. 2, *a*, *b*. The equations for the frequency and voltage controllers according to Fig. 2, *a* are defined by

$$f^*_{GM} = f_N, \quad f^*_{GS} = f_{nl} + P_{GS}(f_N - f_{nl})/\left(k^*_{ps}P_{GM}\right), \quad U^*_{GM} = U_N, \quad U^*_{GS} = U_{nl} + Q_{GS}(U_N - U_{nl})/\left(k^*_{qs}Q_{GM}\right), \quad (1)$$

where $k^*_{ps}$, $k^*_{qs}$ are the reference ratios of the active and reactive power of the slave-generator (SlG) to the active and reactive power of the MG; $f^*_{GM}$, $U^*_{GM}$ are the frequency and voltage reference of the MG; $f^*_{GS}$, $U^*_{GS}$ are the frequency and voltage reference of the SlG; $f_N$, $f_{nl}$ are the rated frequency and no load frequency; $U_N$, $U_{nl}$ are therated voltage and no load voltage; $P_{GM}$, $Q_{GM}$ are the active and reactive power of the MG.

If the control variables for the frequency and voltage controllers of the SU are instantaneous power components of the MG (Fig. 2, *b*), then the equations of these controllers are given by

$$P^*_{GS} = \begin{vmatrix} 0, P_{GM} < P_{\text{cut in}} \\ k^*_{ps}P_{GM}, P_{GM} \geq P_{\text{cut in}} \end{vmatrix}, \quad Q^*_{GS} = \begin{vmatrix} 0, Q_{GM} < Q_{\text{cut in}} \\ k^*_{qs}Q_{GM}, Q_{GM} \geq Q_{\text{cut in}} \end{vmatrix}, \quad (2)$$

where $P^*_{GS}$, $Q^*_{GS}$ are the active and reactive power reference of the SlG.
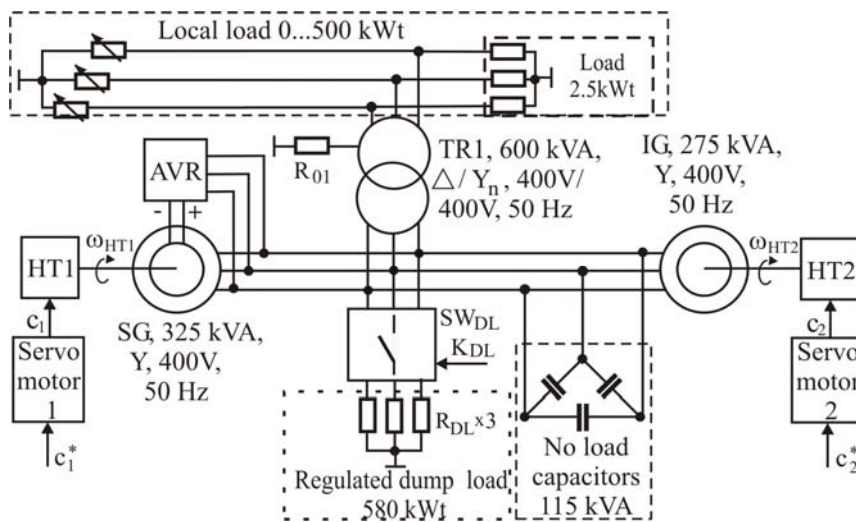


**Fig. 1**
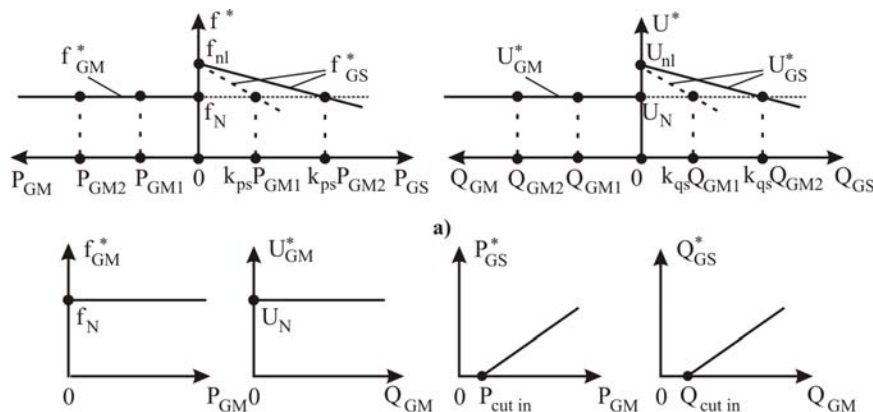
The main feature of the proposed MMGM, that the functions of the voltage and frequency regulation are performed by a subsystem composed of a power unit with a MG, controlled loads with interface converters, such as RDLs, battery inverters, flywheel energy storage systems, etc. All the mentioned elements, except for the power unit with the MG, are not able to seperately or in conjunction with each other provide a long-term sustainable power supply of consumers with the necessary voltage parameters. According to the classic MGM, the functions of frequency and voltage regulation in an IPS are performed only by the MU. In accordance with the MMGM, contrary to the MGM, continuous or discontinuous assistance in the frequency and voltage regulation to the MG by various elements of the subsystem is possible. Due to this, the quality of frequency and voltage regulation during transients in IPSs can be improved. It is also assumed by



**Fig. 2**

the MMGM that the function of the SU's control system, similarly to the classic MGM, is just a load sharing between the generators.

In accordance with the MMGM the reference curve sets of frequency and voltage controllers were obtained for the system "SG – RDL – IG" (Fig. 3, a, b).

The Fig. 3, a curves are defined by:

$$f_{DL}^* = f_N, \quad U_{GM}^* = U_N, \quad P_{GM}^* = k_{PM}^*(P_{01} + P_{\Sigma L}), \quad P_{GS}^* = k_{PS}^*(P_{01} + P_{\Sigma L}), \quad P_{GM}^* + P_{GS}^* > P_{\Sigma L}, \quad (3)$$

where $f_{DL}^*$ is the frequency reference of the RDL frequency controller; $U_{GM}^*$ is a terminal voltage reference of the MG, $P_{01} = P_{0M} + P_{0S} = const$ is a frequency-responsive fast reserve of active power in the system; $P_{\Sigma L}$ is a total active load demand; $k_{PM}^*$, $k_{PS}^*$ is a reference load sharing coefficients of the generators, $k_{PM}^* + k_{PS}^* = 1$. In the steady-state of diesel sets and hydraulic units the fuel consumption and water flow rates can approximately be considered proportional to the active power of the generators. Accordingly, the reference values of the fuel consumption or water flow rates can be obtained from (3) as:

$$q_M^* = k_{qpM}k_{PM}^*(P_{01} + P_{\Sigma L}), \qquad q_S^* = k_{qpS}k_{PS}^*(P_{01} + P_{\Sigma L}), \qquad (4)$$

where $q_M^*$, $q_S^*$ are the master-unit and slave-unit fuel consumption or water flow rate reference; $k_{qpM}$, $k_{qpS}$ are the flow rate to active power ratios of the master and slave units in steady state (fixed speed operation).

The equations of frequency and voltage controllers according to Fig. 3, b are given by:

$$P_{DL}^* = const \; if \; f_l < f < f_h, f_{DL}^* = f_l \; if \; f < f_l, f_{DL}^* = f_h \; if \; f > f_h, U_{GM}^* = U_N, f_{GM}^* = f_N, P_{GS}^* = k_{S/M}P_{GM}^*, (5)$$

where $P_{DL}^*$ is the RDL power reference; $f_l$, $f_h$ are the lower and upper permissible limits of the operating range of the electrical frequency in the system, $f_l < f_N < f_h$; $k_{S/M}$ is the reference value of active power of the SlG related to the active power of the MG. If the load sharing in proportion to the rated powers of the generators is necessary, then the $k_{S/M}$ value must be taken equal to the ratio of the rated powers of the SlG and MG.
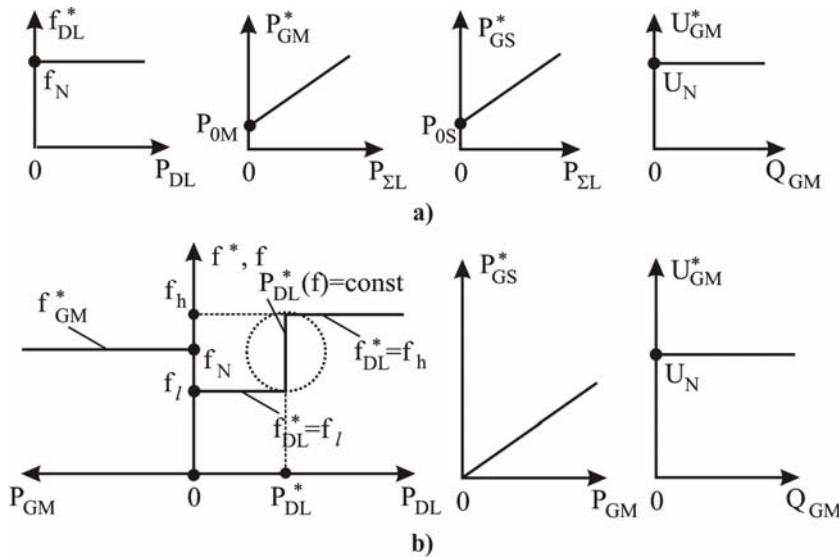


**Fig. 3**

Adding in (5) the flow rate to active power ratio coefficient of the SU $k_{qpS}$ gives:

$$q_S^* = k_{qpS}k_{S/M}P_{GM}^*. \quad (6)$$

If the prime movers of the generators are of the same type and have similar mechanical power – flow rate (fuel consumption) characteristics, then the value of $q_S^*$ can be defined as $q_S^* = k_{S/M}q_M^*$ or in p.u. units by:

$$q_{S(p.u.)}^* = k_{S/M(p.u.)}q_{M(p.u.)}^*, \quad (7)$$

where $k_{S/M(p.u.)}$ is the reference value of the p.u. active power of the SlG related to the p.u. active power of the MG; $q_{S(p.u.)}^*$, $q_{M(p.u.)}^*$ are the MU and SU p.u. fuel consumption or water flow rate.

As seen from (7), for arbitrary power ratings of generators in the system, the condition of active power sharing among the generators proportional to their power ratings is $k_{S/M(p.u.)} = 1$.

It can be seen from (5) that the RDL controller keeps the RDL power value equal to $P_{DL}^*$ when the electrical frequency in the IPS is in the permissible range to maintain a frequency-responsive fast "spinning" reserve of active power in the IPS (RDL controller operates in power regulation mode). If the frequency leaves the limits $f_l \ldots f_h$, then the RDL controller starts operation in the frequency regulation mode.

**Testing of frequency and voltage regulators by simulation of the IPS.** To test the proposed new approaches for frequency and voltage regulation, a simulation model of the IPS of Fig. 1 was developed.

In the simulation model of the IPS of Fig. 1, SG and IG dynamic models of the 6th and 4th order, respectively, were used [4, 22]. The equations of the HT with servo motor are given in [10]. The three-phase transformer was modeled by three single-phase transformers with no magnetic coupling between the phases. The simulation was carried out in Matlab/Simulink environment.

Frequency and voltage control algorithms were implemented based on the system of equations (5, 7). The SG voltage was regulated according to the standard IEEE algorithm [23]. The SG excitation system according to this algorithm maintains the SG terminal voltage value $U_{GM}$ equal to nominal voltage $U_N$ with no voltage droop in the steady state.

A proposed block diagram of speed control of the MU and SU of the Fig. 1 IPS configuration is shown Fig. 4, $a$. The input of this modified PID speed controller of the HT speed governor is the speed error of the MG. The outputs of this controller are the WG p.u. reference angles $c_1^*$ and $c_2^*$ of the hydroelectric units. The coefficient $k_{S/M(p.u.)}$ sets, as mentioned above, p.u. active power value of the IG related to the p.u. active power of the SG. A feature of the controller is that the integrator resets its output to the value of the $c_1^*$ external signal ($c_1^*$ is saved) when the signal on the RES input rises from zero to positive. The rising edge appears every time when crossing the limits $\omega_l - \Delta h_\omega \ldots \omega_h + \Delta h_\omega$ of the HT1 turbine's permissible rotational speed is detected, where $\omega_h = 2\pi f_h / p$, $\omega_l = 2\pi f_l / p$, $\Delta h_\omega = 2\pi \Delta h_f / p$, $p$ is the number of pole pairs, $\Delta h_\omega$, rad/s is the width of the hysteresis band of the window comparator WC1, $\Delta h_f$ is the width of the



**HT1, HT2 control**     **Dump load control**

a)                                          b)
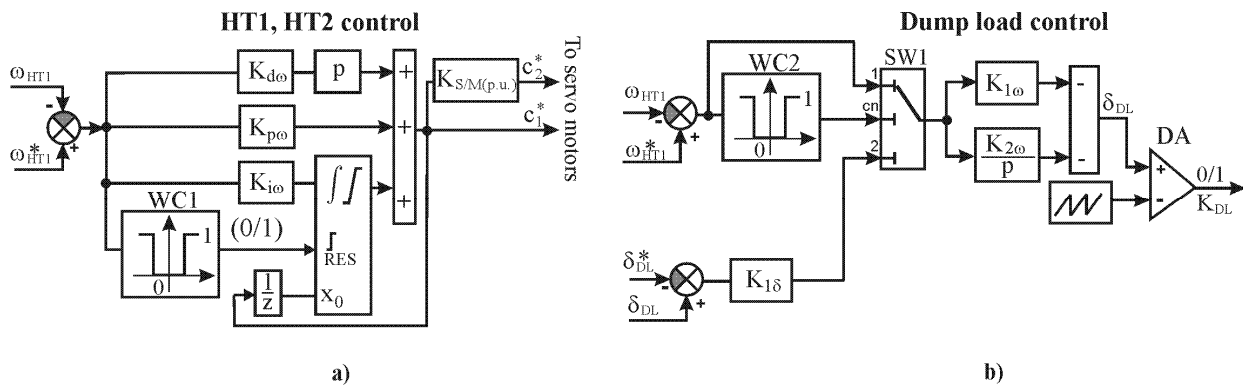
**Fig. 4**

hysteresis band, Hz. This approach affords to reduce the duration of electromechanical transients in the system.

The developed control algorithm of the frequency (power) controller of the RDL's control system is illustrated by Fig. 4, $b$. The controller operates with the rotational speed error signal of the MG if the frequency is outside the permissible limits. If the frequency is within the permissible limits the being used input variable for the controller is the duty cycle error $\delta_{DL} - \delta_{DL}^*$ of the control signal of the SW$_{DL}$ three-phase power switch (Fig. 1). Selection of the first or second input variable is made using the switch SW1 and the window comparator WC2. If the rotational speed of the HT1 turbine leaves the limits $\omega_l - \Delta h_\omega \ldots \omega_h + \Delta h_\omega$, then the signal "1" is set at the output of the WC2 comparator and input 1 of the SW1 switch is connected to its output. The output signal of the SW1 switch is then amplified by the PI controller and passes to one of the inputs of the comparator DA. The other input of the comparator is connected to a sawtooth signal generator. The output signal of the DA comparator is the control signal for the SW$_{DL}$ three-phase power switch. As a result, when the rotational speed of the HT1 turbine is outside the $\omega_l - \Delta h_\omega \ldots \omega_h + \Delta h_\omega$ band, the frequency control loop is activated and the duty cycle value $\delta_{DL}$ is adjusted so that to return the frequency value to the permissible operating band. As soon as the frequency value is within $\omega_l - \Delta h_\omega \ldots \omega_h + \Delta h_\omega$, the signal level at the output of the WC2 comparator will change from "1" to "0" and input 2 of the switch SW1 will be connected to the output of this switch. As a result, the duty cycle

$\delta_{DL}$ control circuit will become active and the $\delta_{DL}$ signal will approach the $\delta_{DL}^*$ value in order to maintain the reference value of the frequency-responsive power reserve in the system.

Verification of the developed control algorithms was carried out by analyzing the electromechanical processes in the system after a 10 % stepwise increase in the resistive local load (Fig. 5). At the same time, the amount of frequency-responsive fast reserve of active power in the steady state was maintained equal to 16 % of the RDL's rated power.

As can be seen from Fig. 5, at first, the IPS supplied a 0.1173 p.u. load, and the power consumption of the RDL was 0.158 p.u. The rotational frequency values of the SG and IG were 1.001 and 1.005 p.u. respectively. The WG angle values in both units were equal to 0.248 p.u. The SG and IG supplied accordingly 0.249 p.u. and 0.26 p.u. of active power into the system. The reactive power value produced by the SG was 0.003 p.u., and the reactive power consumption value of the IG was 0.408 p.u. The difference between the reactive powers of the IG and SG was supplied by the compensating (no load) capacitors.

At the time $t = 15.93\,s$, the local load increased stepwise by a 10 % of the nominal value up to 0.218 p.u. and the rotational speed of both generators started to decrease. As soon as the electrical frequency of the system (the p.u. electrical frequency value equals the p.u. rotational speed value of the SG) decreased to a value lower than $f_l - \Delta h_f = 0.99 - 0.004$ p.u., the frequency control loop of the RDL was activated and a quick decrease of power consumption of the RDL was observed. This, in turn, caused an increase in the rotational frequency of the SG. As soon as the electrical frequency exceeded the value $f_l$, the power control loop of the RDL was activated. The power control loop activation caused an increase in the duty cycle value of the control signal of the SW$_{DL}$ power switch and an increase of power consumption of the RDL. Due to this at the time $t = 19.52\,c$ the electric frequency of the system decreased again to a value lower than $f_l - \Delta h_f = 0.99 - 0.004$ p.u., and, accordingly, the frequency control loop of the RDL controller was activated again. As can be seen
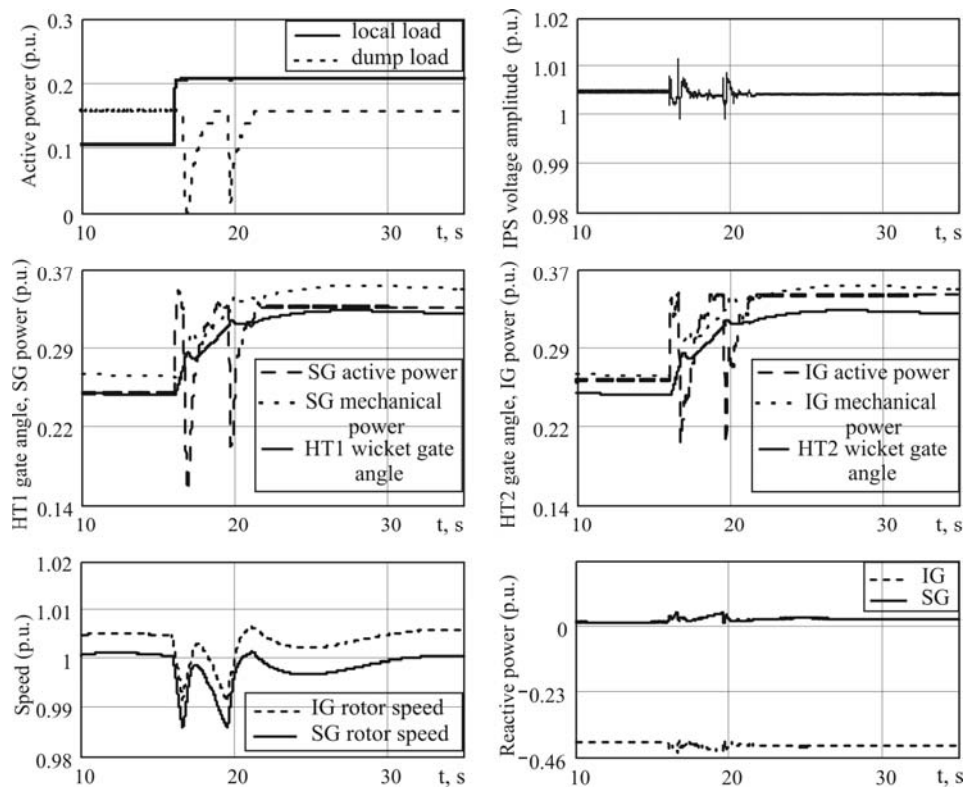


**Fig. 5**

from Fig. 5, when the bang-bang frequency control by the RDL control system was performed, the WG angles, mechanical and active powers of the hydraulic units was growing. As a result of two consecutive activations of the frequency control loop of the RDL control system, the IPS passed to a steady state. The maximum deviation of the electrical frequency from the nominal value did not exceed 1.55%. In the steady state, as seen from Fig. 5, the rotational speed of the SG and, accordingly, the electrical frequency of the system are in the permissible limits. The transients in the IPS died within $15\,s$. This value is several times lower than the die off times of the isolated hydraulic power systems with no RDL. The mean rms voltage value in the system in steady state was 1.005 p.u. The rms voltage deviations from the mean value did not exceed 0.6 %.

**Simulation parameters and characteristics.** _Synchronous generator_. Number of pole pairs – 2. Rated power / frequency / line voltage (connection) – 325 kVA / 50 Hz / 400 V (Y). d, q – axes synchronous

reactances, p.u. – 2.52, 2.16. d – axes transient reactance, p.u. – 0.17. d, q – axes subtransient reactances, p.u. – 0.12, 0.3. Leakage reactance, p.u. – 0.06. Inertia constant (total SG and HT1), s – 2. Stator winding resistance – 0.018 p.u. Short circuit time constants, s: d – axes transient – 0.08, d, q – axes subtransient – 0.019, 0.019. Friction coefficient, p.u. – 0.0167 p.u.

*Induction generator.* Number of pole pairs – 2. Rated power / voltage / frequency (connection) – 275 kVA / 400 V / 50 Hz (Y). Resistance of the stator/rotor winding, p.u. – 0.016/0.015. Stator/rotor leakage inductance – 0.06/0.06 p.u. Inertia constant (total IG and HT2) – 2 s. Friction coefficient – 0 p.u. The magnetization characteristic of the IG is given in the table

| $I_{ph}$, [p.u.] | 0.13 | 0.25 | 0.34 | 0.46 | 0.7 | 1.02 | 1.43 | 2.03 | 2.76 | $U_{LL}$, [p.u.] | 0.67 | 0.86 | 0.96 | 1.05 | 1.15 | 1.25 | 1.34 | 1.44 | 1.5 |
|---|---|---|---|---|---|---|---|---|---|---|---|---|---|---|---|---|---|---|---|

*TR1 transformer.* Rated power/frequency/connection – 600kVA/50Hz/($\Delta$-$Y_n$). Rated line voltage of the primary/secondary windings, V – 400 /400. Resistance of the primary / secondary windings, p.u. – 0.0008/0.0008. Leakage inductance of the primary/secondary windings, p.u. – 0/0. Magnetizing inductance, p.u. – 150. Magnetizing resistance, p.u. – 300.

*Hydro turbines.* Rated power, kW: HT1 – 325, HT2 –275 kW. Turbine gain: HT1, HT2 – 1.073. Damping coefficient: HT1, HT2 – 0. Water starting time, s: HT1, HT2 – 1 s. Servomotor gain: HT1, HT2 – 3.33. WG and servo motor time constant, s: HT1, HT2 – 0.07. No load flow: HT1, HT2 – 0. Head loss due to friction effects in the conduit: HT1, HT2 – 0. Gate opening speed limits, p.u./s: HT1, HT2 – ±0.2. Proportional/integral/differential gains of the PID governor – $k_{p\omega}$ = 1.56/ $k_{i\omega}$ = 0. 48/ $k_{d\omega}$= 0. 62. $k_{S/M(p.u.)}$ =1.

*Dump load.* Rated voltage/power/connection – 400V/580 kW/$Y_n$. Switching frequency, kHz – 5. Off /on-state resistance of the $SW_{DL}$ power switch per phase – 0.001 Ohm / 100 kOhm. Gain coefficients of the frequency (power) controller of the RDL: proportional – $k_{1\omega}$= 0.0012, integral – $k_{2\omega}$ = 0.0493, gain of the power control loop – $k_{1\delta}$=4.

*Local consumer load.* Rated power/power factor – 500 kW/1.

*Base quantities of power, voltage and frequency for Fig. 5 data.* 275 kVA=1 p.u. of the IG's power. 325 kVA=1 p.u. of the SG's power. 500 kW=1 p.u. of the consumer load. 580 kW=1 p.u. of the RDL's power. 400 V=1 p.u. of voltage. 1500 rpm=1 p.u. of rotational speed.

*Compensating capacitors.* Rated power/rated voltage/connection: 115kVA/400V/$Y_n$.

**Conclusions.** The proposed MMGM is intended for voltage and frequency regulation with no droop in IPSs with parallel operated var compensators, regulated loads, energy storage devices, intermittent power sources and AC electric generators driven by prime movers with regulated mechanical torque (hydro turbines, etc.). This method involves the joint regulation of the frequency and/or voltage by two or more elements of the system, one of which is the master generator control system, and the others are controllers of the interface power converters of the RDLs, energy storage devices, var compensators and intermittent generation sources. One of the two presented systems of equations for frequency and voltage controllers based on the statements of the proposed method was used in the developed simulation model of a 500 kW hydraulic IPS with parallel operated SG, IG and RDL of alternating current. The results of simulation studies have shown that the developed block diagrams of the HT speed control and the RDL frequency (power) control provide simultaneously reference electric frequency tracking and maintenance of the required amount of frequency-responsive fast reserve of active power in the system.

1. Sebastián R., Nevado A. Study and Simulation of a Wind Hydro Isolated Microgrid. *Energies.* 2020. No 13. Pp. 1-15. DOI: https://doi.org/10.3390/en13225937.

2. Mazurenko L.I., Dzhura O.V., Kotsiuruba A.V.,Shykhnenko M.O. A Wind-Hydro Power System Using a Back-to-Back PWM Converter and Parallel Operated Induction Generators. IEEE *Problems of Automated Electrodrive. Theory and Practice (PAEP).* Kremenchuk, Ukraine, September 21-25, 2020. Pp. 1-5. DOI: https://doi.org/10.1109/PAEP49887.2020.9240777.

3. Hatata A.Y., El-Saadawi M.M., Saad S. A feasibility study of small hydro power for selected locations in Egypt. *Energy Strategy Reviews.* 2019. Vol. 24. Pp. 300-313. DOI: https://doi.org/10.1016/j.esr.2019.04.013.

4. Kundur P., Neal J. Balu, Mark G. Lauby Power System Stability and Control. New York: McGraw-Hill, 1994. 1176 p.

5. Grebenikov V.V., Gamaliia R.V. Comparative Analysis of Two Types of Generators with Permanent Magnets for Wind Turbine. IEEE International Conference on *Modern Electrical and Energy Systems (MEES).* Kremenchuk, Ukraine, September 23-25, 2019. Pp. 126-129. DOI: https://doi.org/10.1109/MEES.2019.8896375 .

6. Mazurenko L.I., Vasyliv K.M., Dzhura O.V., Kotsiuruba A.V. Simulation model and control algorithm for isolated hydro-wind power system. *Tekhnichna Electrodynamika*. 2020. No 1. Pp. 17-26. DOI: https://doi.org/10.15407/techned2020.01.017 (Ukr).

7. Shapoval I.A., Mykhalskyi V.M., Artemenko M.Y., Chopyk V.V., Polishchuk S.Y. Compensation of Current Harmonics by means of Multiple Generation System with Doubly-Fed Induction Generators. IEEE 7th International Conference on *Energy Smart Systems (ESS)*. Kyiv, Ukraine, May 12-14, 2020. Pp. 26-29. DOI: https://doi.org/10.1109/ESS50319.2020.9160238.

8. Wang G., Zhai Q., Yang J. Voltage control of cage induction generator in micro hydro based on variable excitation. International Conference on *Electrical Machines and Systems.* Beijing, China, 20-23 August 2011. Pp. 1-3. DOI: https://doi.org/10.1109/ICEMS.2011.6073988.

9. Babunski D., Tuneski A. Modelling and design of hydraulic turbine-governor system. IFAC Workshop on *Automatic Systems for Building the Infrastructure in Developing Countrie. 2003*. Vol. 36. No 7. Pp. 263-267. DOI: https://doi.org/10.1016/S1474-6670(17)35842-1 .

10. Mazurenko L.I., Kotsiuruba A.V., Dzhura O.V., Shykhnenko M.O. Voltage and Power Regulation of an Induction Generator-Based Hydroelectric Power Plant. IEEE International Conference on *Modern Electrical and Energy Systems (MEES)*. Kremenchuk, Ukraine, 21-24 September 2021. Pp. 1-6. DOI: https://doi.org/10.1109/MEES52427.2021.9598549.

11. Janardhan Reddy V., Singh S.P. Voltage and frequency control of parallel operated synchronous and induction generators in micro hydro scheme. *2014 International Conference on Computation of Power, Energy, Information and Communication (ICCPEIC)*. Chennai, India, 16-17 April 2014. Pp. 124-129. DOI: https://doi.org/10.1109/ICCPEIC.2014.6915352.

12. Vanço W.E., Silva F.B., Gonçalves F.A.S., Silva E.O., Bissochi C.A., Neto L.M. Experimental analysis of a self-excited induction generators operating in parallel with synchronous generators applied to isolated load generation. *IEEE Latin America Transactions*. 2016. Vol. 14. No 4. Pp. 1730-1736. DOI: https://doi.org/10.1109/TLA.2016.7483508.

13. Torque Angle versus Load or Power Angle. URL: https://electengmaterials.com/torque-angle-versus-load-or-power-angle/ (accessed at 30.04.2022).

14. Mobarak Youssef. SVC, STATCOM, and transmission line rating enhancments on induction generator driven by wind turbine. *International Journal of Electrical Engineering and Technology (IJEET)*. 2012. Vol. 3. Issue 1. Pp. 326-343.

15. Abdessemad O., Nemmour A.L., Louze L., Khezzar A. An Experiment Validation of an Efficient Vector Control Strategy for an Isolated Induction Generator as Wind Power Conversion. International Conference on *Advanced Electrical Engineering (ICAEE)*. Algiers, Algiera, 19-21 November 2019. Pp. 1-5. DOI: https://doi.org/10.1109/ICAEE47123.2019.9014784.

16. Shurub Y., Vasilenkov V. Elimination of self-oscillation mode in a thyristor-controlled induction electric drive. IEEE 2nd KhPI Week on *Advanced Technology (KhPI Week).* Kharkiv, Ukraine, 13-17 September 2021. Pp. 585-588. DOI: https://doi.org/10.1109/KhPIWeek53812.2021.9570081.

17. Butkevych O.F., Chyzhenko O.I., Popovych O.M., Trach I.V. An influence of the facts upon an electrical network's mode during direct start-up of an asynchronous machine in the complex load's composition. *Tekhnichna Electrodynamika.* 2018. No 6. Pp. 62-68. DOI: https://doi.org/10.15407/techned2018.06.062.

18. Rain A., Saritac M.E. Estimation and Prediction Optimization of Hydropower System Planning with FuzzyNeural Networks based on Genetic Algorithm. *Computational Research Progress in Applied Science & Engineering (CRPASE): Transactions of Electrical, Electronic and Computer Engineering.* 2021. No 7. Pp. 1-9. DOI: https://doi.org/10.52547/crpase.7.2.2351.

19. Levshov A.V. Basics of automation of energy systems: learning aid. DonNTU, 2005. URL: https://studfile.net/preview/5685918/ (accessed at 07.06.2022) (Rus).

20. Verma Kunal Subhash, Ashish Aboti. Review on Industrial Generators Load Sharing System Along Withgrid Momentry Synchronization and Setup a Backup Unit for Auxiliary Power for Generators. *International Journal For Technological Research In Engineering*. 2018. Vol. 5. Iss. 8. Pp. 3448–3456. URL: https://ijtre.com/wp-content/uploads/2021/10/2018050816.pdf (Accessed at 03.08.2022).

21. Andoni Urtasun, Pablo Sanchis, Luis Marroyo. State-of-Charge-Based Droop Control for Stand-Alone AC Supply Systems with Distributed Energy Storage. *Energy Conversion and Management*. 2015. Vol. 106. Pp. 709-720. DOI: https://doi.org/10.1016/j.enconman.2015.10.010.

22. Krause Paul C., Wasynczuk O., Scott D. Sudhoff. Analysis of Electric Machinery and Drive Systems. Wiley-IEEE Press, 2002. 632 p. DOI: https://doi.org/10.1109/9780470544167.

23. 421.5-1992 – IEEE Recommended Practice for Excitation System Models for Power System Stability Studies. 1992. Pp. 1-56. DOI: https://doi.org/10.1109/IEEESTD.1992.106975.

## РОЗВИТОК МЕТОДУ ВЕДУЧОГО ГЕНЕРАТОРА ДЛЯ РЕГУЛЮВАННЯ ЧАСТОТИ І НАПРУГИ В АВТОНОМНИХ СИСТЕМАХ ЕЛЕКТРОЖИВЛЕННЯ З ПАРАЛЕЛЬНО ПРАЦЮЮЧИМИ ГЕНЕРАТОРАМИ ЗМІННОГО СТРУМУ

**Л.І. Мазуренко**[1], докт.техн.наук, **О.В. Джура**[1], канд.техн.наук, **М.О. Шихненко**[1], канд.техн.наук, **А.В. Коцюруба**[2]
[1] Інститут електродинаміки НАН України,
просп. Перемоги, 56, Київ, 03057, Україна.　　　　　　　**E-mail:　mlins@ied.org.ua.**
[2] Національний університет оборони ім. Івана Черняховського,
Повітрофлотський просп., 28, Київ, 03049, Україна.

*Методи статичних характеристик, уявностатичних характеристик та ведучого генератора розроблялися для регулювання напруги і частоти в автономних системах електроживлення, побудованих на основі синхронних генераторів. В сучасних системах електроживлення крім синхронних генераторів застосовують також асинхронні генератори, регульовані баластні навантаження, накопичувачі енергії з AC/DC та AC/DC/AC напівпровідниковими перетворювачами, тощо. Дослідження нових конфігурацій автономних систем електроживлення тісно пов'язано з подальшими розробками методів регулювання розподілу навантаження та частоти і напруги. В статті розглянуті прості в реалізації відомі методи регулювання систем з паралельно працюючими синхронними генераторами та розвинуто метод ведучого генератора для автономних систем з паралельно працюючими синхронними і асинхронними генераторами, статичними компенсаторами реактивної потужності, регульованими баластними навантаженнями та накопичувачами енергії з інтерфейсними напівпровідниковими перетворювачами. Розглянуто автономну систему «Гідроагрегат з синхронним генератором – баластне навантаження – гідроагрегат з асинхронним генератором – батарея компенсуючих конденсаторів – трансформатор – навантаження змінного струму» та запропоновано на основі положень розвинутого методу два підходи до регулювання електричної частоти і напруги в зазначеній системі. Розроблений алгоритм роботи регулятора частоти системи керування баластним навантаженням узгоджується з алгоритмом роботи регулятора частоти ведучого гідроагрегату. Функції стабілізації електричної частоти системи на номінальному рівні та розподілу активного навантаження в системі покладено на ПІД-регулятор частоти обертання ведучого гідроагрегату. Проведено верифікацію запропонованих алгоритмів керування частотою автономних систем електроживлення. Бібл. 23, рис. 5, табл. 1.*

**Ключові слова**: автономна система електроживлення, метод, ведучий генератор, ведений генератор, баластне навантаження.